CHAPTER 7

Microstructure and Mechanical Behaviour of SiO_2 Coated ABO_w-Al Composites

In this investigation, the powder metallurgy route has been employed to synthesize the SiO_2 (5, 10, and 15% Vol.) coated ABO_w/Al composites. The commercial pure aluminium powder was used as matrix material, and SiO_2 coated ABO_w was used as reinforcements [125-130]. The microstructures of composites were characterized using scanning electron microscopy (SEM) and high resolution scanning electron microscopy (HRSEM). Energy dispersive spectroscopy (EDS) was employed to confirm the weight percentages of elements present in the composites. Transmission electron microscopy (TEM) analysis was performed for the observation of morphological changes in the composites. The XRD analysis was carried out to confirm the phases of developed reinforcement and composites. A universal testing machine observed the flexural strengthand diametral compressive strength of fabricated composites. Young's modulus of the samples after immersion for different durations was calculated. Properly cleaned samples after being removed from SBF were taken Young's modulus calculations. For testing the samples for calculating Young's modulus, ultrasonic testing of the composite was done by the non-destructive testing (NDT) method [77]. In the NDT method for Young's modulus calculations, the longitudinal and transverse wave was measured with the aid of ultrasonic gauge (45 MG, Olympus, USA). The effects of SiO_2 coating on ABO_w fabricated composites were evaluated and found that the hardness value is 46.2 Hv in 10 Wt% SiO_2 coated.

7.1 Phase identification and microstructural examination

7.1.1 Phase identification of fabricated composites

XRD pattern of aluminium matrix composites samples sintered in the range of 600°C is shown in **Figure 7.1**. It shows that except for aluminium, SiO_2, and ABO_w, no other phases were present in the composites fabricated. As the volume content of coated ABO_w increases, the height of aluminium peaks decreases, whereas the height of ABO_w peaks increases.

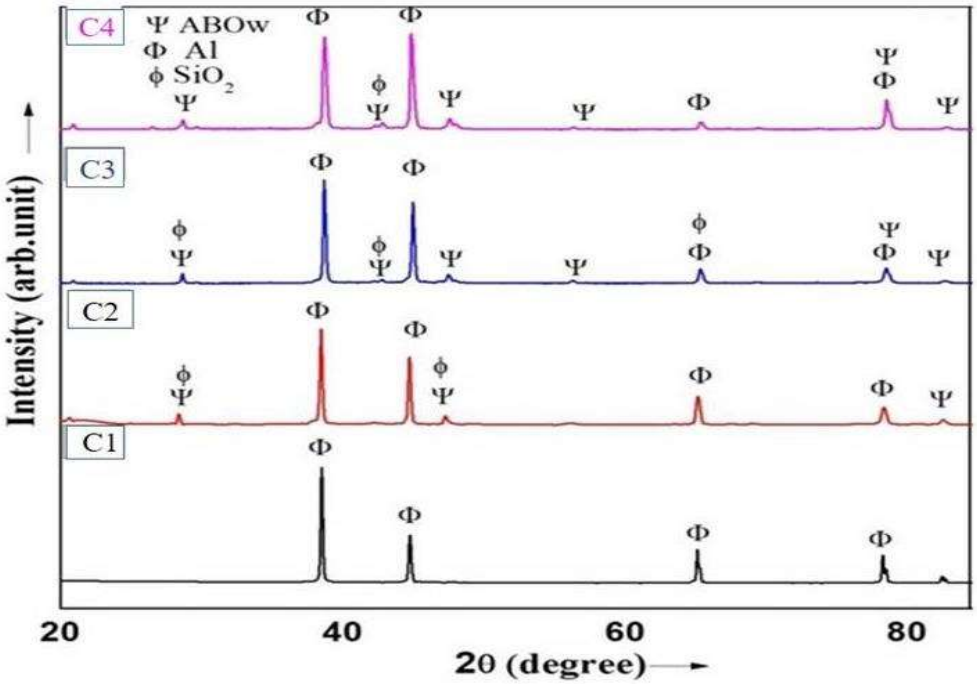

Figure 7.1: XRD patterns of SiO_2 coated composite sintered at 600° C for 2 h with different composition

7.2.2. Electron microscopy

The SEM micrographs are shown in **Figure 7.2** for all sintered composites and reinforcement respectively. The distribution of ABO_w whiskers can be seen throughout the volume of cast composites. However, increasing the whisker percentage causes

agglomeration of whiskers and composite to become more porous as shown in **Figure 7.2 (d).**

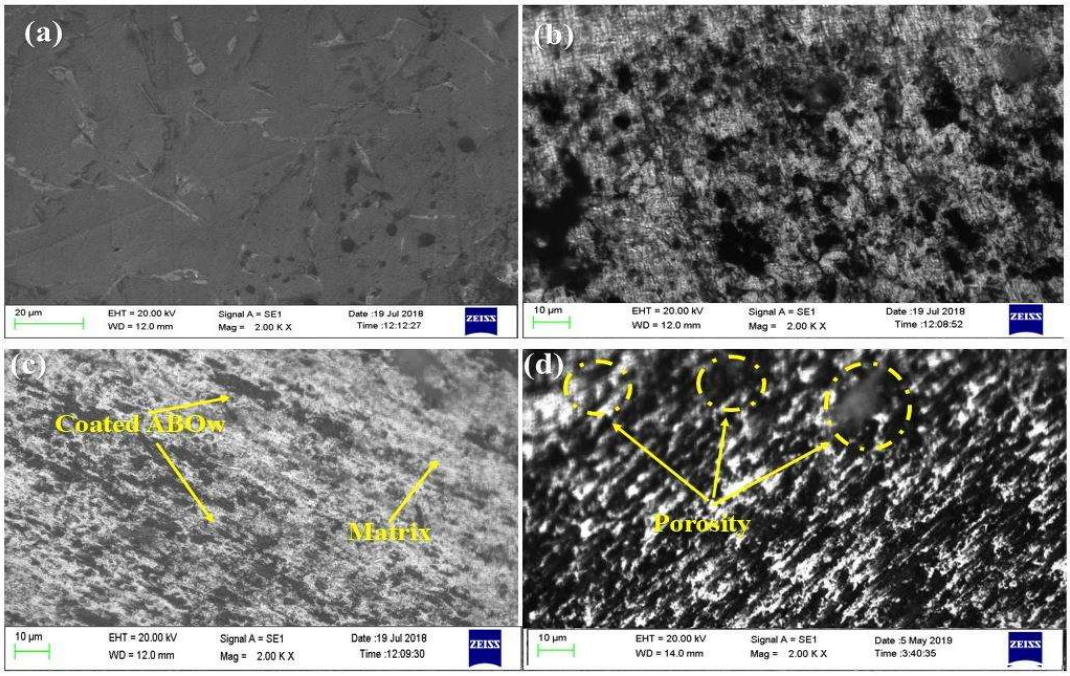

Figure 7.2: SEM micrographs of **(a)** pure Al **(b)** composite with SiO_2 coated 5 wt% ABO_w (C1) **(c)** composite with SiO_2 coated 10 wt% ABO_w (C2) **(d)** composite with SiO_2 coated 15 wt% ABO_w (C3) sintered at 600°C

The TEM bright-field images with corresponding selected area diffraction patterns (SADP) of ABO_w powder are shown in **Figure 7.3**. The crystal parameters of whiskers have already been determined as a=7.6874 Å, b=15.0127 Å, and c=5.6643Å. The parameters confirm the orthorhombic structure of ABO_w reinforcements, as shown in **Figure 7.3 (a)** already discussed in our previous chapter. The whisker was observed to be a needle-like crystal with smooth surfaces (thickness ~20 µm) and no cavities. **Figure 7.3 (b)** shows typical ABO_w/Al composites reinforced with coated SiO_2

whiskers. It can be seen that the SiO_2 coatings are almost uniformly deposited on whisker surfaces with a thickness of about 20–50 nm.

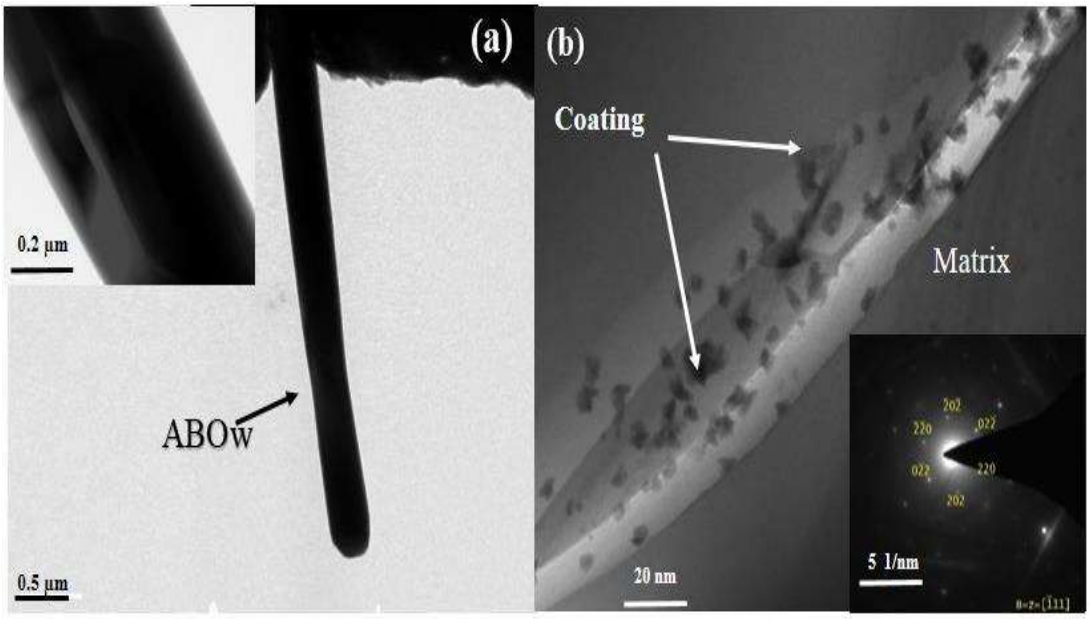

Figure 7.3: (a) Bright field Image of coated ABO_w and higher magnification ABO_w (inset) **(b)** bright-field image of ABO_w/Al and corresponding SAED (inset) of composite sintered at 600°C

Figure 7.4 (b) shows typical ABO_w/Al composites reinforced with coated SiO_2 whiskers. It can be seen that the SiO_2 coatings are almost uniformly deposited on whisker surfaces with a thickness of about 20–50 nm. Due to clean and fine SiO_2 surfaces, the whisker surface was observed to be clean and zig-zag. In contrast, it is also observed that there is no interfacial reaction occurs between composites constituents and a clean interface made between ABO whisker and pure aluminium.

The specific region's energy dispersive spectrometry shows that the whisker surface in **Figure 7.4 (c)** without coated alumina borate and **Figure 7.4 (d)**. It clearly shows the presence of SiO_2 thin layer, confirming the coating on alumina borate whisker.

It was confirmed that tight interface bonding also occurred between the whiskers and SiO_2 particles.

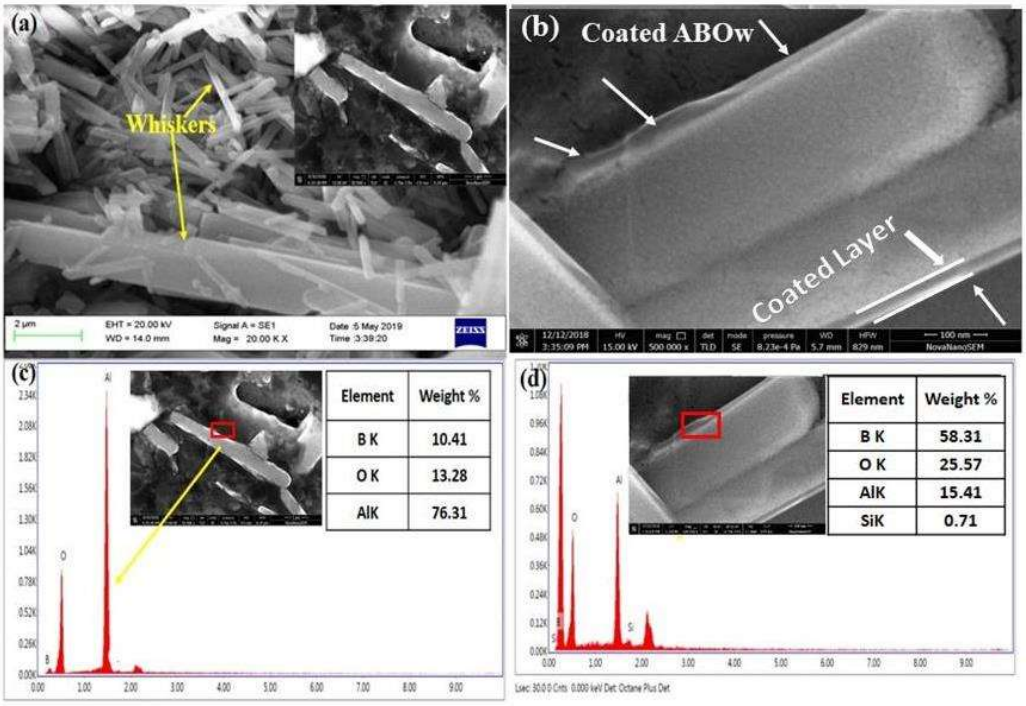

Figure 7.4: HRSEM image of reinforcement **(a)** calcined at 1300°C without coated ABO_w corresponding single whisker (inset) **(b)** coated ABO_w calcined at 1100 °C **(c)** corresponding EDS of uncoated whisker **(d)** corresponding EDS of coated whisker

7.2. Porosity analysis

From **Table 7.1,** it can be observed that the density of the specimens decreases with increasing the volume fraction of whiskers in the aluminium matrix. It shows the micro-sized whiskers decrease the density of the specimens with an increased percentage in a matrix. Also, the increased percentage of whiskers increases the average porosities in the sintered composites. Although composite with coated 15 wt.% ABO_w shows increased porosity percentage due to the more interlocking and rounded shape of whiskers.

Table 7.1. Average % porosity of Al matrix and composites

Composites	Sample Number	Experimental density(g/cc)	Theoretical density ($\rho_{th}=V_f\rho_f+V_m\rho_m$)	Average porosity (%)
Base Al	1	2.58	2.70	4.43
	2	2.55		
	3	2.57		
C1	1	2.49	2.65	6.28
	2	2.50		
	3	2.46		
C2	1	2.38	2.67	9.72
	2	2.43		
	3	2.60		
C3	1	2.10	2.13	11.72

7.3 Mechanical characterization

7.3.1 Vicker's hardness and flexural strength

Microhardness measurements were performed for three samples of each composite and their average value has been taken, the sample was done using a Vicker's hardness tester of 1kg load. The hardness and flexural strength are shown in **Figure 7.5**. The samples' hardness increases by increasing the percentage of whiskers in the matrix. The hardness of base Al composites C1, C2 and C3 were calculated as 27 Hv, 39.9 Hv, 46.2 Hv, and 41 Hv, respectively. This may be due to inhibition of the progress of plastic deformation by whiskers present in the matrix. As agglomeration of whiskers proceeds in specimens with 15 wt% ABO_w, the non-uniform sintering leads to localized shrinkage strains that may introduce more defects (dislocations and point defects, etc.) at the interfaces of ABO_w and matrix during grain growth, so the interface strength decreases

during sintering. This behaviour of composite increases with increasing volume fraction of coated ABO_w in the aluminium matrix.

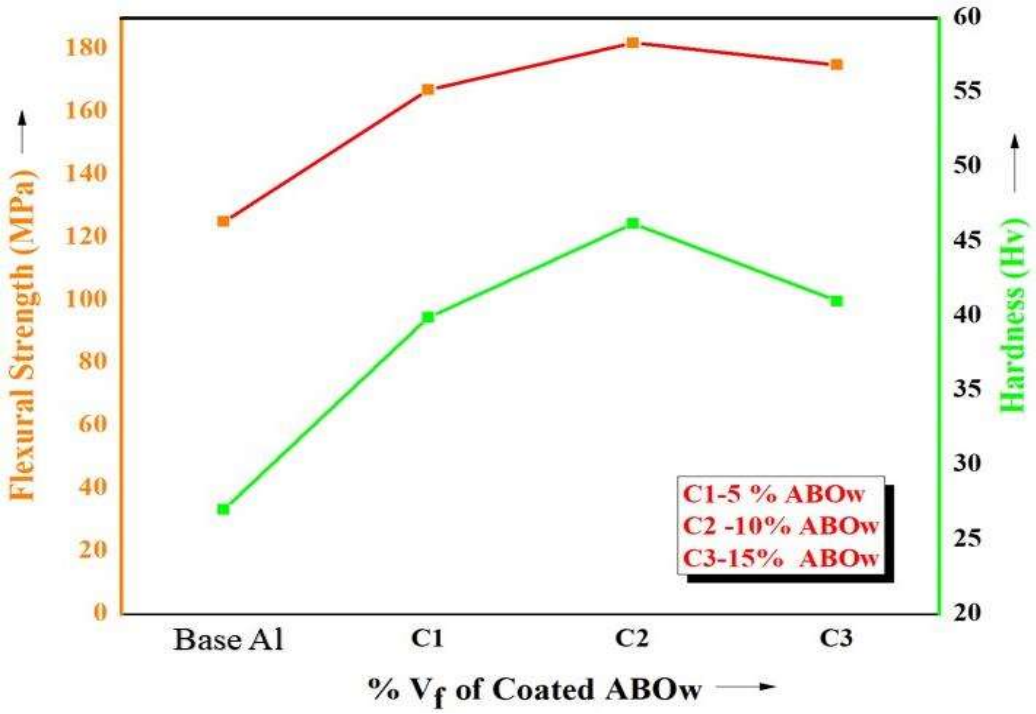

Figure 7.5: Measurement of flexural strength and hardness of base Al and composites sample sintered at 600°C

The flexural strength of the metal matrix composite reinforced with SiO_2/ABO_w depends upon the whiskers' matrix type, whisker aspect ratio, and volume fraction. The three-point bending test was employed for measuring the flexural strength of given samples having a span length of 30 mm and a crosshead speed of 0.5mm/min. The values obtained for the base Al, samples C1, C2 and C3 were 125 MPa, 167 MPa, 182 MPa and 175 MPa, respectively. It was found that the highest flexural strength 182 MPa was obtained in sample C2.

7.3.2 Diametral compression behaviour and Young's modulus

The diametral compression test and Young's modulus were performed for three samples and their average value has been taken for more accurate results.

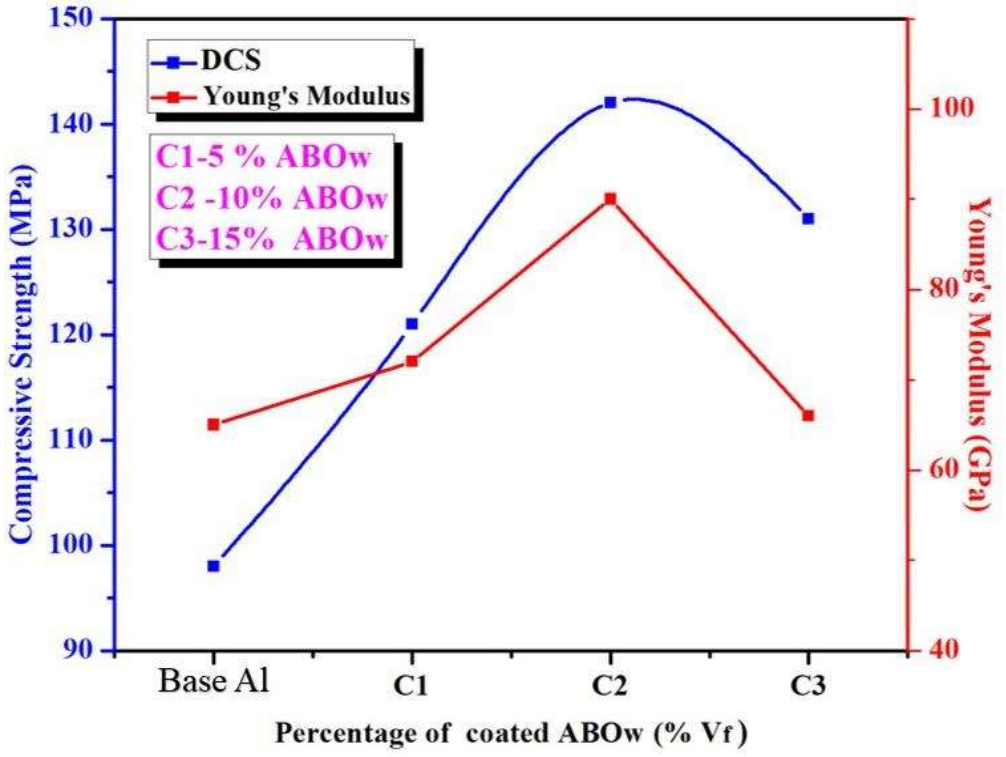

Figure 7.6: Diametral compressive strength of sintered sample at 600°C base Al and composites

Figure 7.6 shows the change in the strength of specimens with varying percentages of coated ABO whisker in the sample. In the case of composites structures, it is equally important to find out a DCS for their requirements in structural applications. The diametral compressive load depends on the materials and flow stress behavior. By establishing a relationship between flow stress and strain, the flow behaviour of aluminium composites can be determined at different compositions. The variation of wt% of coated ABO_w on DCS and Young's modulus of elasticity of aluminium matrix composites are shown in **Figure 7.6**. DCS value increases with increasing the wt%. For sample C2, DCS (142 MPa) was obtained, which is higher than that obtained for the base aluminium (98 GPa), sample C1 (121 MPa), and C3 (131 MPa). It may be observed that an increase in wt % of reinforcement in the matrix inhibited grain boundary formation, slowed down dislocation motion, and prevented grain growth.

These phenomena led to an increase in the strength of the specimen. Improvement of DCS has excellent importance from the viewpoint of stiffness design, making the SiO_2 coated ABO_w-Al composites suitable materials for gas and oil pans, engine crankcase, and lightweight structural application.

Table 7.2 Young's modulus of elasticity of sintered sample

S.N.	Sample Name	Transverse ultrasonic wave velocity V_S (µm/sec)	Longitudinal ultrasonic wave velocity V_L (µm/sec)	V_S /V_L	σ	E (GPa)
1	Base Al	3.82	5.91	0.66	0.33	65
2	C1	4.12	6.23	0.67	0.33	70
3	C2	5.31	7.12	0.74	0.33	89
4	C3	4.92	6.91	0.77	0.33	67

The Young's modulus of the sintered samples of the base alloy was 65 GPa. The values of V_L and V_S for calculating Young's modulus of the sintered sample and those of SiO_2 coated ABO_w reinforcement has been shown in **Table 7.2**. The Young's modulus of the samples increases with an increase in coated ABO_w content, their values being in the range of 70-89 GPa. However, it decreases for sample C3, which may be due to an increase in the percentage of whisker content and agglomeration in the matrix. Also, the increasing percentage and non-homogeneous distribution of porosity affect the diametral compressive strength in sample C3.

7.4. Fracture surface analysis

7.4.1 Fractograph of flexural test

The micrograph of fractured surfaces of sintered composites after the flexural test is analyzed with SEM as shown in **Figure 7.7**. After the flexural test at room temperature, the fractured surface of aluminium alloy shows a ductile nature along the micro-holes on the surface and whisker-free weak areas in the composite as presented in **Figure 7.7 (a)**. The fractography of SiO_2 coated ABO_w/Al composites as shown in **Figure 7.7 (b), (c)** and **(d)** shows a brittle nature of fracture specifically at whisker and matrix interface. Better bonding between matrix and whisker led to excellent flexural strength to the composite because load may be distributed from matrix to the whisker.

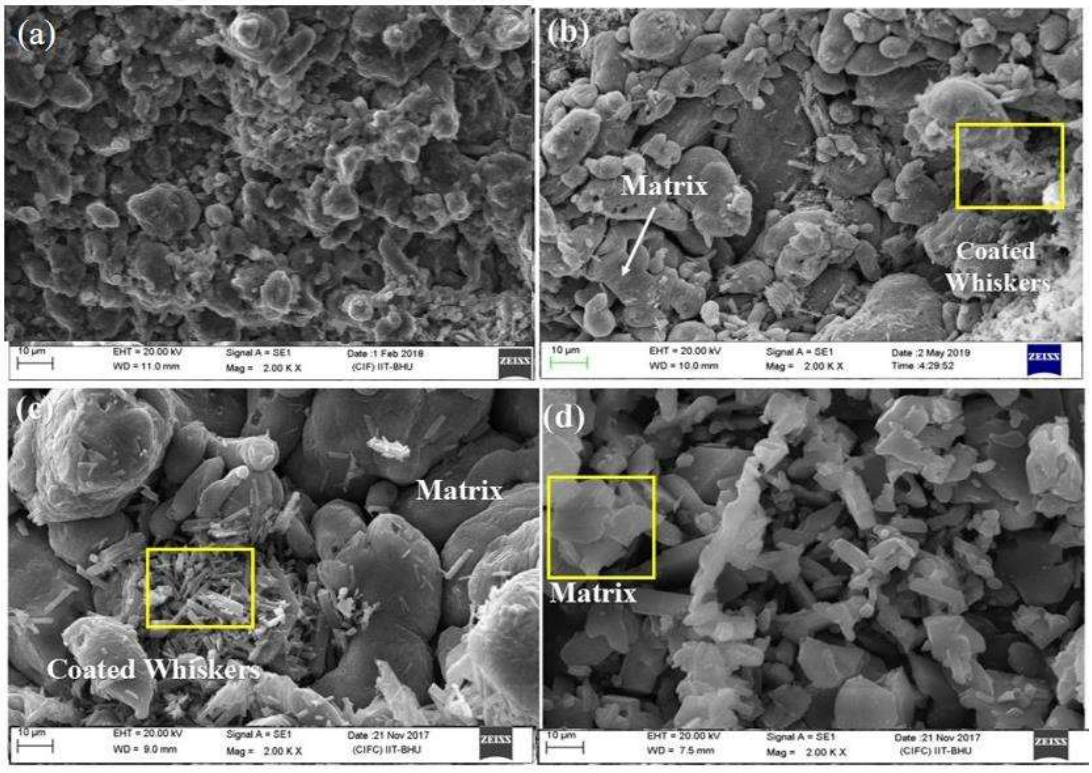

Figure.7.7: The SEM micrograph of fractured surface (a) pure aluminium (b) composite with SiO_2 coated 5 wt% ABO_w (C1) (c) 10 wt% ABO_w (C2) (d) 15 wt % ABO_w (C3) sintered at 600°C

Figure 7.7 (c) shows most of the whiskers pullout from the matrix during a mechanical test due to lower interfacial bonding and high brittleness. However, **Figure 7.7 (d)** shows more agglomerates of aluminium matrix on the fracture surface. The introduction of SiO_2 coatings to the whisker-reinforced composite has hindered the strength-decrease effect due to the weakening of matrix alloys.

7.4.2 Fractograph of diametral compression test

DCS test photographs of sintered samples at 600°C as shown in **Figure 7.8**. The images of different samples compositions are shown in **Figure 7.8 (a)** before the diametral compression test setup image is shown in **Figure 7.8 (b)**, and the image of the compressed pellet after the DCS test is presented in **Figure 7.8 (c)**. The SEM was carried out for the fracture behavior of tested samples of diametric compression test as shown in **Figure 7.8 (d)**. Resultantly it was found that a diametric crack reflects on surfaces. SEM analysis of the fracture surfaces was further carried out to observe fracture behavior and found that most of the surfaces show a localized cracks that causes the samples were broken entirely down through without subsequent transfer of load into the specimen [132-134]. It is well known that the type of interface between the matrix and reinforcement plays an essential role in stress transfer, thus affecting the mechanical properties of the composites. The fractography of samples after the diametral compression test is shown in **Figure 7.9**. It was observed that in sample C1 the presence of voids around the whiskers was minimum on the surface, indicating unfilled regions of the matrix due to less volume fraction of whiskers, as shown in **Figure 7.9 (a)**. Fractography as shown in **Figure 7.9 (b)** of sample C2 shows that most of the whiskers pull out from the matrix and may affect the mechanical strength. Sample C3 surface

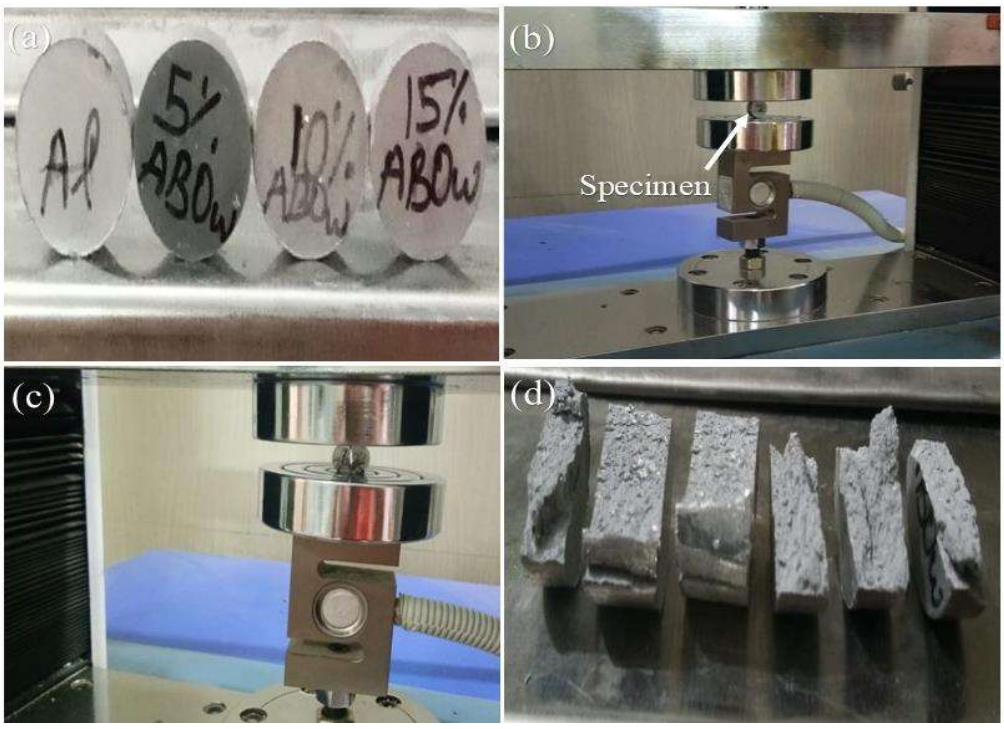

Figure 7.8: Photographs of the sintered pallet at 600°C of (a) different composition (b) before diametral compression test (c) compressed pallet (d) fractured pallet after the diametral compression test

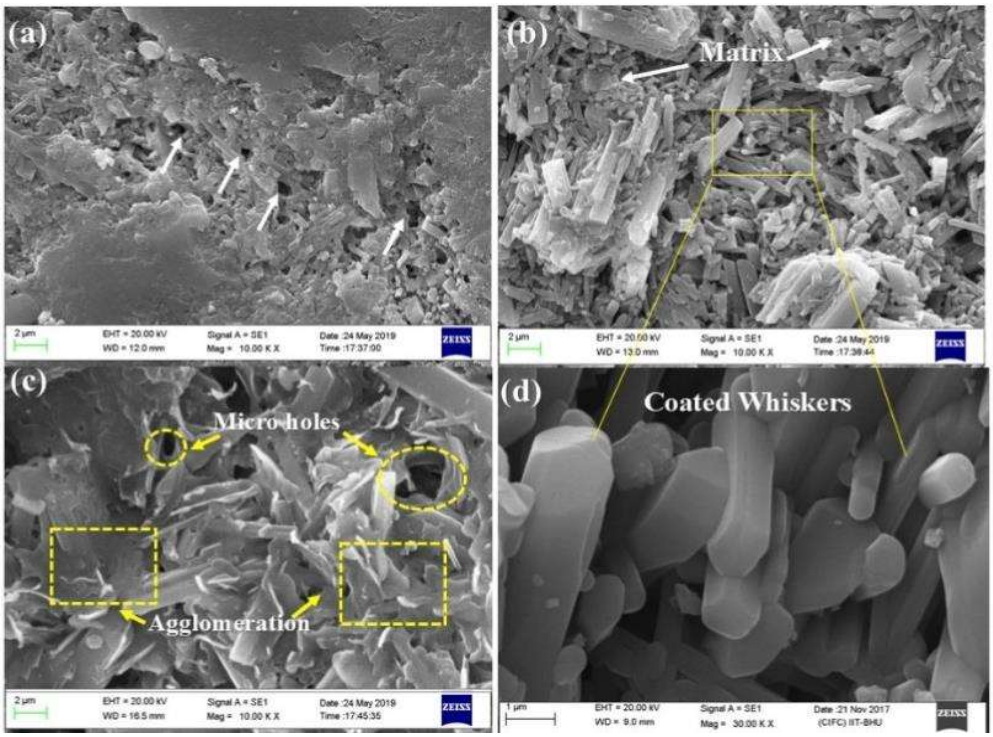

Figure 7.9: The SEM micrograph of factured surface after DCS test (a) composite with SiO_2 coated 5wt% ABO_w (C1) (b) 10 wt % ABO_w (C2) (c) 15 wt% ABO_w (C3) (d) high magnification SEM image of SiO_2 coated whisker

reflected agglomerated whiskers, micro holes and voids indicating sample fractured through brittle mode refer **Figure 7.9 (c)**.

7.5 Chapter summary

In this chapter, SiO_2 coated Al-ABO_w metal matrix composite has been synthesized using a powder metallurgy route. After physical and mechanical characterizations and the analysis of their results, we have found the hydrolyzation method for preparation of coated ABO_w reinforcement and powder metallurgy route for the development of Al-coated ABO_w based composites has been successfully approached for this investigation.

The SEM, HR-SEM were used for microstructures observations, i.e. phases and grain structure are clearly observed. It is also found that the distribution of ABOw particles is almost uniform. TEM analysis showed the rod-like structures and observed the single-crystal morphologies of ABO_w particles along with the discontinuous structure of the micro whiskers with the matrix. SiO_2 is the strongest because of high density and low porosity at 1100 °C cristobalite phase is formed as seen in XRD which is very dense.

The density of the composite decreases with an increasing percentage of whisker in the matrix. The microhardness of composite improved in SiO_2 coated 10 wt% ABO_w/Al (C2) with reduced porosity and better bonding between matrix and reinforcement.

The maximum flexural strength around 182 MPa and DCS 142 MPa with SiO_2 coated 10 wt% ABO_w(C2) reinforcement was observed. The Young's modulus of the samples was obtained in 65-89 MPa for sample C2. Flexural strength and DCS of SiO_2

coated ABO_w was seen to be significantly improved than aluminium as a base alloy. This can be attributed to the presence of a reasonably uniform distribution of coated whiskers. Fractography of fractured surfaces shows the debonding of the particle due to detachment of coated ABO_w from the matrix and shows whiskers are unbreakable under the application of load.